Linear-fitting-based similarity coefficient map for tissue dissimilarity analysis in T_2^*-w magnetic resonance imaging*

Yu Shao-De(余绍德)[a)b)], Wu Shi-Bin(伍世宾)[a)b)], Wang Hao-Yu(王浩宇)[c)], Wei Xin-Hua(魏新华)[d)], Chen Xin(陈 鑫)[d)], Pan Wan-Long(潘万龙)[e)], Hu Jiani[f)], and Xie Yao-Qin(谢耀钦)[a)†]

[a)] *Shenzhen Institutes of Advanced Technology, Chinese Academy of Sciences, Shenzhen* 518055, *China*

[b)] *University of Chinese Academy of Sciences, Beijing* 100049, *China*

[c)] *Department of Experimental Pathology, Beijing Institute of Radiation Medicine, Beijing* 100049, *China*

[d)] *Department of Radiology, Guangzhou First Hospital, Guangzhou* 510080, *China*

[e)] *Institute of Medical Imaging, North Sichuan Medical University, Nanchong* 637007, *China*

[f)] *Department of Radiology, Wayne State University, Detroit* 48201, *USA*

(Received 3 April 2015; revised manuscript received 4 August 2015; published online 20 October 2015)

Similarity coefficient mapping (SCM) aims to improve the morphological evaluation of T_2^* weighted magnetic resonance imaging (T_2^*-w MRI). However, how to interpret the generated SCM map is still pending. Moreover, is it probable to extract tissue dissimilarity messages based on the theory behind SCM? The primary purpose of this paper is to address these two questions. First, the theory of SCM was interpreted from the perspective of linear fitting. Then, a term was embedded for tissue dissimilarity information. Finally, our method was validated with sixteen human brain image series from multi-echo T_2^*-w MRI. Generated maps were investigated from signal-to-noise ratio (SNR) and perceived visual quality, and then interpreted from intra- and inter-tissue intensity. Experimental results show that both perceptibility of anatomical structures and tissue contrast are improved. More importantly, tissue similarity or dissimilarity can be quantified and cross-validated from pixel intensity analysis. This method benefits image enhancement, tissue classification, malformation detection and morphological evaluation.

Keywords: T_2^*-w magnetic resonance imaging, similarity coefficient map, linear fitting, tissue dissimilarity

PACS: 87.61.–c, 87.57.C–, 02.10.Ud **DOI:** 10.1088/1674-1056/24/12/128711

1. Introduction

Signal correlation analysis from tissue similarity (or dissimilarity) plays an important role in medical image analysis, such as tissue classification and segmentation,[1–3] functional region localization,[3–5] morphological evaluation,[6–8] abnormality detection,[8–10] and others.[11–13]

As to similarity coefficient mapping (SCM), it is a post-processing method and analyzes signal correlation from tissue similarity.[6] It enhances visual perceptibility of anatomical structures and helps clinical diagnosis with improved morphological evaluation. Also, it can compress a T_2^*-w magnetic resonance image series into a map which shows high image quality and non-sensitivity to the choice of reference tissues. In SCM maps, small structures, such as minor veins which are hard to distinguish from surroundings in original T_2^*-w magnetic resonance images, are clearly observed in *in vivo* study and thus the accuracy of morphological evaluation of hemorrhage and pseudo-capsule of renal cancer is improved.

Wang *et al.*[6] has fully demonstrated how to derive the similarity map and what is the effect of the selection of the reference tissue and the echo number on map quality. However, how to interpret the SCM map is still unknown. In addition, is it probable to extract tissue dissimilarity messages based on the theory behind SCM? The purpose of this paper is to answer these two questions.

The rest of this paper is arranged in the following way. Section 2 interprets SCM from linear fitting and then extends it with an additional term to release tissue dissimilarity information into another map. Besides, the derivation of our newly proposed method and the experiment design are introduced. In Section 3, experimental results are evaluated in terms of signal-to-noise ratio (SNR) and perceived visual quality, and investigated from intra- and inter-tissue pixel intensity analysis. Discussion and conclusion of this study are presented in Sections 4 and 5, respectively.

*Project supported in part by the National High Technology Research and Development Program of China (Grant Nos. 2015AA043203 and 2012AA02A604), the National Natural Science Foundation of China (Grant Nos. 81171402, 61471349, and 81501463), the Innovative Research Team Program of Guangdong Province, China (Grant No. 2011S013), the Science and Technological Program for Higher Education, Science and Research, and Health Care Institutions of Guangdong Province, China (Grant No. 2011108101001), the Natural Science Foundation of Guangdong Province, China (Grant No. 2014A030310360), the Fundamental Research Program of Shenzhen City, China (Grant No. JCYJ20140417113430639), and Beijing Center for Mathematics and Information Interdisciplinary Sciences, China.

†Corresponding author. E-mail: yq.xie@siat.ac.cn

© 2015 Chinese Physical Society and IOP Publishing Ltd

2. Method and material

2.1. Improved similarity coefficient mapping

SCM measures relative signal magnitude between a tissue of interest (TOI) and a selected reference tissue. To a stationary subject, an image series

$$I = \{I_1, \ldots, I_n\}$$

is acquired with n-echo T_2^*-w MRI and images are spatially aligned with ascending echo time (TE). Accordingly, there is a row vector of pixel intensities $V_{ij} = \{V_{ij1}, \ldots, V_{ijn}\}$ for a position (i, j), while the reference signal

$$R = \{R_1, \ldots, R_n\}$$

is constructed by averaging pixel intensities in the selected tissue region. SCM takes advantage of the mean square error (MSE) to compute the relatedness between V_{ij} and R in the following equation,

$$\mathrm{MSE}_{ij} = \frac{1}{n}\sum_{k=1}^{n} ||V_{ijk} - \lambda_{ij} R_k||^2, \tag{1}$$

where λ_{ij} stands for the relative signal magnitude. Tissue dissimilarity information is valuable in tissue classification and segmentation[2] and malformation detection.[8–10] In dynamic imaging, it was also used to uncover invisible hemodynamic responses and local pharmacokinetics.[1,3–5,11,12] In such a case, a term ε_{ij} is added to release this kind of message in multi-echo T_2^*-w magnetic resonance image series

$$\mathrm{MSE}_{ij} = \frac{1}{n}\sum_{k=1}^{n} ||V_{ijk} - \lambda_{ij} R_k - \varepsilon_{ij}||^2. \tag{2}$$

With known signal R and V_{ij}, let

$$\frac{\partial MSE_{ij}}{\partial \lambda_{ij}} = 0$$

and

$$\frac{\partial \mathrm{MSE}_{ij}}{\partial \varepsilon_{ij}} = 0$$

for MSE_{ij} minimization.

$$\frac{\partial \mathrm{MSE}_{ij}}{\partial \lambda_{ij}} = -\frac{2}{n}\sum_{k=1}^{n} (V_{ijk} - \lambda_{ij} R_k - \varepsilon_{ij}) R_k = 0, \tag{3}$$

$$\frac{\partial \mathrm{MSE}_{ij}}{\partial \varepsilon_{ij}} = -\frac{2}{n}\sum_{k=1}^{n} (V_{ijk} - \lambda_{ij} R_k - \varepsilon_{ij}) = 0. \tag{4}$$

From Eq. (4), we get

$$\varepsilon_{ij} = \frac{1}{n}\sum_{k=1}^{n} V_{ijk} - \lambda_{ij}\frac{1}{n}\sum_{k=1}^{n} R_k = \overline{V_{ij}} - \lambda_{ij}\overline{R}. \tag{5}$$

Substituting Eq. (5) into Eq. (3), we obtain

$$\lambda_{ij} = \frac{\overline{V_{ij}R'} - \overline{V_{ij}} \cdot \overline{R}}{\overline{RR'} - (\overline{R})^2}. \tag{6}$$

In Eqs. (5) and (6), "$\overline{(\ )}$" denotes the average value of a vector in ( ) and "R'" stands for the transpose of vector R. With these two equations, λ_{ij} and ε_{ij} to each signal at (i, j) can be calculated and two maps are respectively constructed in a pixel-wise computation. Please note that, in our method, the derived map from λ_{ij} is marked as the relative magnitude map (RMM), and the map from absolute value of ε_{ij} is marked as the residual map (RM). Also, to each image series, the derived RMM and RM make up a map pair for further investigation.

It is found that SCM and iSCM can be interpreted from the perspective of linear fitting and the theory behind them can be expressed as

$$V_{ij} = f(R) = \lambda_{ij} R$$

and

$$V_{ij} = f(R) = \lambda_{ij} R + \varepsilon_{ij},$$

respectively. Therefore, we can conclude that: if one signal is similar to the reference tissue signal, its value on RMM should be about 1 (it is the same interpretation to SCM) and its corresponding value on RM will be near 0. In other words, tissue similarity or dissimilarity can be quantified and cross-validated with the generated map pair.

2.2. *In vivo* study

Four volunteers participated and were scanned with a 3.0 Tesla scanner (SIEMENS) with gradient-echo MRI pulse sequence (flip angle: 15°; field of view: 220 mm × 220 mm; image matrix: 384 × 384; slice thickness: 3.0 mm; slice gap: 0.9 mm; repetition time: 200 ms). TE values range from 2.61 ms to 38.91 ms with an equal interval 3.3 ms. Four paralleling brain sections were scanned from each of these four volunteers (aged 22, 23, 25, and 29). Taken together, sixteen T_2^*-w magnetic resonance image series were collected.

2.3. Experiment design

Local cerebral-spinal fluid (CSF) and white matter (WM) tissue regions are delineated by Wei Xin-Hua (an expert radiologist from Guangzhou first Hospital, Guangzhou, China) as TOIs, and these TOIs act as the reference signal one after another. In addition, when one TOI works as the reference tissue, we will name the other one as the non-reference.

This study mainly focuses on generated map pairs from iSCM. First, the signal-to-noise ratio is quantified as $\mathrm{SNR} = \mu_{\mathrm{roi}}/\delta_{\mathrm{air}}$, where μ_{roi} and δ_{air} stand for the mean value and the standard deviation value of pixel intensities in the TOI and the air region, respectively. An air region of 60 × 60 pixels is outlined in each image series and the size of TOI is 6 × 6 pixels. For each T_2^*-w magnetic resonance image series, the maximum signal-to-noise ratio ($\mathrm{SNR}_{\mathrm{max}}$) of each TOI is defined as

the baseline for comparison. Then, tissue similarity or dissimilarity is observed from the map pair and finally interpreted from intra- and inter-tissue pixel intensity investigation.

3. Results

3.1. Signal-to-noise ratio analysis

These four volunteers are indexed with V1, V2, V3, and V4 for distinction and sixteen T_2^*-w magnetic resonance image series are analyzed. For each image series, a map pair is generated from iSCM by taking the TOI of CSF or WM region to form the reference signal. For each volunteer, average SNR values of TOIs are shown in Table 1.

For each TOI in Table 1, $\mathrm{SNR_{max}}$ stands for the maximum SNR in original magnetic resonance images, $\mathrm{SCM_{csf}}$, $\mathrm{RMM_{csf}}$, and $\mathrm{RM_{csf}}$ indicate SNR values in the generated maps with TOI of CSF to form the reference signal, while $\mathrm{SCM_{wm}}$, $\mathrm{RMM_{wm}}$, and $\mathrm{RM_{wm}}$ are SNR values in the map with TOI of WM as the reference. In addition, lower SNR values in RM are highlighted in bold.

Table 1. Average SNR values of tissues of interest (CSF and WM) in generated maps.

	TOI	$\mathrm{SNR_{max}}$	$\mathrm{SCM_{csf}}$	$\mathrm{RMM_{csf}}$	$\mathrm{RM_{csf}}$	$\mathrm{SCM_{wm}}$	$\mathrm{RMM_{wm}}$	$\mathrm{RM_{wm}}$
V1	CSF	44.80	141.50	141.51	**2.85**	138.90	138.33	30.22
	WM	59.21	136.64	136.69	38.46	140.12	140.13	**1.99**
V2	CSF	43.76	136.11	136.12	**3.51**	134.2	133.74	24.19
	WM	50.15	120.54	120.64	26.97	122.59	122.60	**1.89**
V3	CSF	40.95	127.30	127.31	**3.07**	125.28	124.81	21.94
	WM	51.66	123.53	123.61	22.87	125.61	125.59	**1.93**
V4	CSF	42.01	130.35	130.35	**2.87**	128.85	128.43	21.09
	WM	59.98	145.47	145.61	29.14	147.54	147.52	**2.07**

3.2. Perceived visual quality

The third image series of the first volunteer and its derived maps are selected as a representative for visual quality analysis. In Fig. 1, [panels (a), (b), and (c)] respectively show the 1st, the 4th, and the 10th T_2^*-w magnetic resonance image, panels (d), (e), and (f) are derived maps when selecting the TOI of CSF as the reference tissue, while panels (g), (h), and (i) are maps when TOI of WM as the reference tissue. In Fig. 1(c), the delineated CSF, WM and air regions are respectively highlighted with pink, green and red squares. Pixels on blue lines in panels (e), (f), (h) and (i) are for further pixel intensity investigation, and pixels of red circle in CSF region and pixels of green sparker in WM region are for image interpretation based on the theory behind iSCM.

3.3. Image interpretation

Intra- and inter-tissue investigation based on pixel intensity is shown in Fig. 2. In Fig. 2, black dots in panels (a), (b), (c), and (d) respectively correspond to those pixel intensities on the blue lines in Fig. 1 [panels (e), (f), (h), and (i)], and red circles and green sparkers are also in accordance with circles and sparkers in Fig. 1. The baseline of magnitude equal to 1 is indicated by red lines in panels (a) and (c).

4. Discussion

The similarity coefficient mapping is a post-processing method and improves the morphological evaluation in T_2^*-w magnetic resonance images.[6] However, how to interpret the generated SCM map is pending. This paper firstly interpreted the theory of SCM from the perspective of linear fitting and then extended it for tissue dissimilarity messages. Finally, the improved method was validated with *in vivo* study and derived maps were investigated from signal-to-noise ratio and perceived visual quality, and observed from intra- and inter-tissue pixel intensity.

Local tissue region signal-to-noise ratio comparison is shown in Table 1, where relative magnitude map (RMM) exhibits competitive capacity as SCM in signal-to-noise ratio improvement and non-sensitivity to the reference signal, while RM demonstrates high tissue contrast. Comparing $\mathrm{RM_{csf}}$ and $\mathrm{RM_{wm}}$, it is found that the signal-to-noise ratio shows high sensitivity to the choice of the reference tissue and that the signal-to-noise ratio of non-reference tissue region is much higher than signal-to-noise ratio of the reference tissue region. For instance, to V1, when the tissue of interest of CSF performs the reference signal, the signal-to-noise of TOI in WM region in $\mathrm{RM_{csf}}$ (38.46) is about 13.5 times higher than that in CSF region in $\mathrm{RM_{csf}}$ (2.85); but when the tissue of interest of WM works as the reference, the signal-to-noise of TOI in WM region in $\mathrm{RM_{wm}}$ (1.99) is only 6.6% of that in CSF region in $\mathrm{RM_{wm}}$ (30.22). This kind of sensitivity to the reference signal is also uncovered in Figs. 1 and 2.

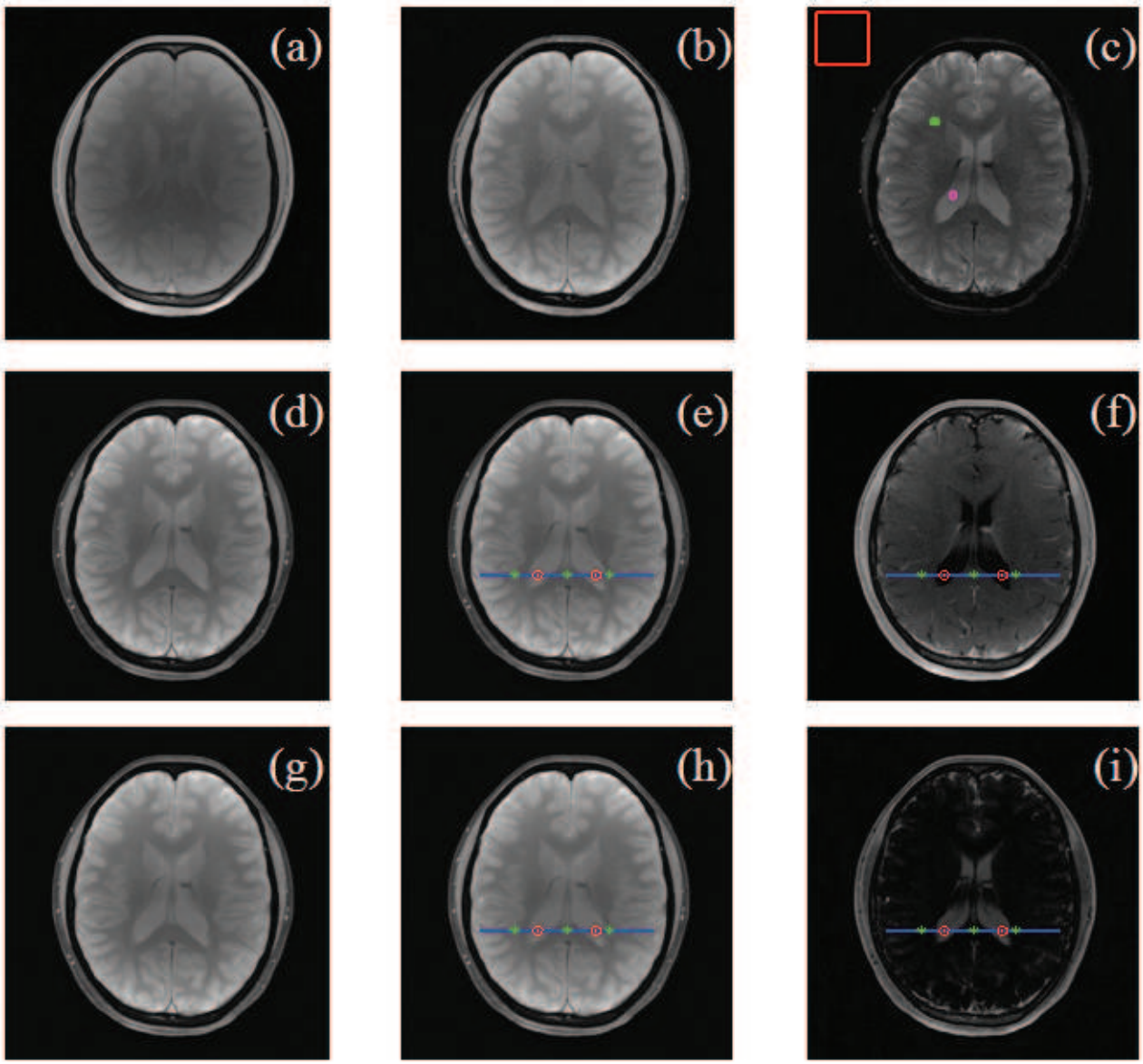


Fig. 1. (color online) Perceived visual image quality analyses. The third image series of the first volunteer and its derived maps are represented. Panels (a), (b), and (c) are T_2^*-w magnetic resonance images with ascending TE value (2.61 ms, 12.51 ms, and 35.61 ms), panels (d), (e), and (f), and panels (g), (h), and (i) are SCM, RMM, and RM maps from tissue of interest (CSF and then WM) as the reference tissue, respectively. Pixels on the blue lines are for further intra- and inter-tissue pixel intensity investigation.

Figure 1 shows visual image quality with one representative. When TE increases, tissue shapes, such as CSF, become much clearer and complete. With different TOIs to construct the reference signal, visual perception of SCM and RMM shows no difference and both enhance perceived quality of anatomical structures. It is found that high tissue contrast is shown in RM maps. When TOI of CSF forms the reference signal (see Fig. 1(f)), the cerebral-spinal fluid region becomes much darker than its surroundings; but when TOI of WM performs as the reference signal (see Fig. 1(i)), pixel intensities in CSF region become much higher. For image interpretation, pixels on blue lines are investigated in Fig. 2, and red circles and green sparkers are highlighted for intra- and inter-tissue pixel intensity analysis.

Medical images are the first-hand materials for image analysis and disease diagnosis[14] and the precise image interpretation plays an important role in clinical applications. As aforementioned in Subection 2.1, theoretically, if one signal is similar to the reference signal, its value on RMM is about 1, and its corresponding value on RM will be close to 0. With this understanding in mind, intra-tissue similarity and inter-tissue dissimilarity can be quantified and cross-validated.

Image interpretation is concerned in Fig. 2. From map pairs of RMM and RM, the rightness of iSCM theory is proved. When TOI of CSF work as the reference, pixel intensities of red circles in CSF region on RMM are close to 1 (see Fig. 2(a)) and on RM are near to 0 (see Fig. 2(b)); when TOI of WM is the reference, pixel intensities of green sparkers

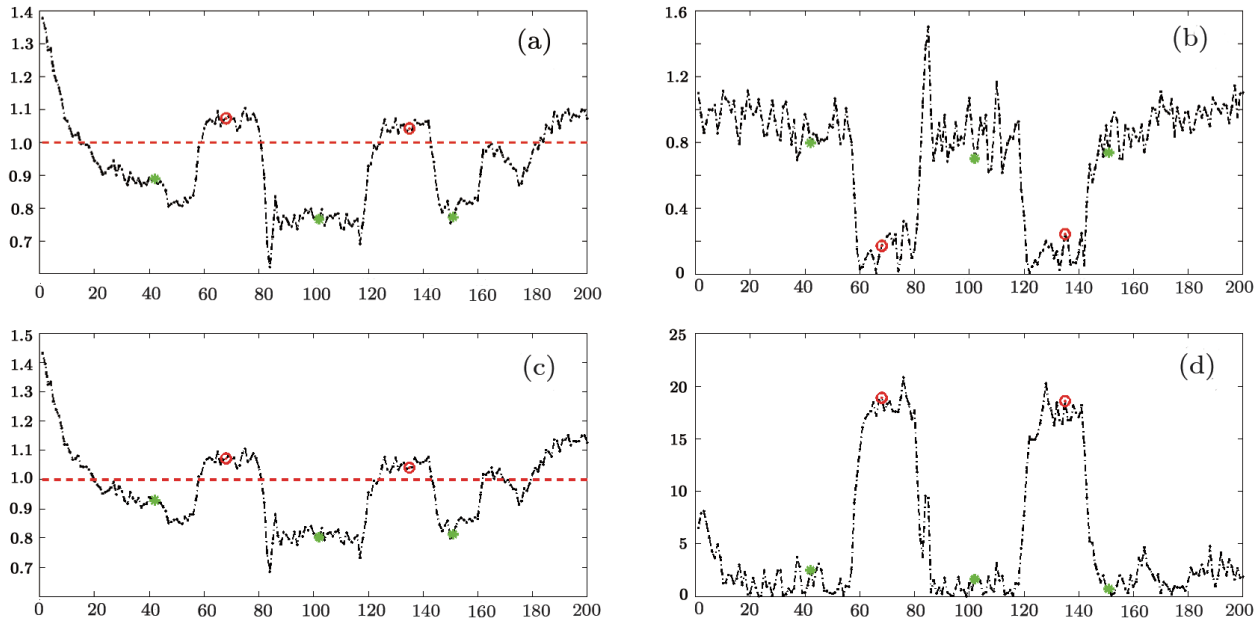


Fig. 2. (color online) Intra- and inter-tissue analysis and theoretical interpretation based on pixel intensity observation. Black dots shown in panels (a), (b), (c), and (d) respectively correspond to those pixel intensities on the blue lines in Fig. 1 [panels (e), (f), (h), and (i)], and red circles and green sparkers are also in accordance. The x axis corresponds to the pixel index and the y axis shows the pixel intensity

in WM region on RMM are shifted toward 1 (see Fig. 2(c)) and on RM are much closer to 0 (see Fig. 2(d)). However, it should be mentioned that, in Fig. 2(c), when taking TOI of WM as the reference tissue, green sparkers indicating WM tissue are slightly away from the baseline. Several reasons are accountable for this kind of ambiguity. Above all, WM and grey matter are adjacent in spatial distribution in the human brain. With limited image resolution, partial volume effects play a major role and thus the reference signal is a mixture and not only purely from WM. In contrast, the cerebral-spinal fluid is more homogeneous and clear CSF shapes and boundaries lead to accurate selection. Moreover, noise, magnetic field inhomogeneity and artifacts are unavoidable in magnetic resonance images which result in the distortion of the reference signal calculation.

Another one that should be mentioned is that, it is hard to tell which one is better between SCM and RMM maps, neither from SNR comparison in Table 1 or from perceived visual quality in Fig. 1. That is because the theory behind SCM and iSCM is similar and both can be interpreted from the perspective of linear fitting. But compared to SCM, one definite advantage of iSCM lies on the RM map which shows high tissue contrast from SNR comparison (Table 1), visual perception (Fig. 1) and pixel intensity investigation (Fig. 2).

In addition, both similarity coefficient mapping and iSCM are targeted to the same tomographic slice, thus the anatomical structures in the image series should remain stationary. If relative motion occurs, spatial alignment is necessary. Meanwhile, correct selection of the reference tissue region is crucial before mapping computation and inaccurate delineation of reference tissue regions is bound to give the wrong map interpretation. In human brain study, the cerebral-spinal fluid is preferable to be the reference tissue. Our study suggests that similarity mapping techniques suppress noise, but this de-noising property does not mean the reduction of partial volume effects nor intensity in-homogeneity nor artifacts.[8]

Except for signal correlation measurements, many other techniques can be borrowed to post-process magnetic resonance image series. One simple way is to average image series. In this manner, the image quality can be improved, but higher tissue contrast is uncertain because of the intrinsic tissue difference. Another way is quantitative magnetic resonance imaging[15] which seeks to quantify fundamental biological messages and MR-inducible tissue properties, such as T_2. Other methods include fuzzy clustering, principal component analysis and image compression.[16–18]

Generally, our method belongs to the category of signal correlation measurement, but it fuses image series into two maps, i.e., RMM and RM. With the generated maps, intra-tissue similarity and inter-tissue dissimilarity can be quantified and cross-validated. Hence, signal investigation, organ localization, tissue classification, malformation detection and morphological evaluation can benefit from this method.

5. Conclusion

In this paper, the similarity coefficient mapping is embedded with an additional term for inter-tissue dissimilarity. With the generated map pair, the intra-tissue similarity and the inter-tissue dissimilarity can be quantified and cross-validated. The

method proposed by us benefits the image fusion, the tissue classification and segmentation, the malformation detection, and the morphological evaluation.

References

[1] Lucas-Quesada F A, Sinha U and Sinha S 1996 *Magn. Reson. Imaging* **6** 753
[2] Wiart M, Rognin N, Berthezene Y, Nighoghossian N, Froment J C and Baskurt A 2001 *Magn. Reson. Med.* **45** 261
[3] Rogowska J, Preston K Jr, Hunter G J, Hamberg L M, Kwong K K, Salonen O and Wolf G L 1995 *IEEE Trans. Med. Imaging* **14** 480
[4] Bandettini P A, Jesmanowicz A, Wong E C and Hyde J S 1993 *Magn. Reson. Med.* **30** 161
[5] Friston K, Jezzard P and Turner R 1994 *Hum. Brain Mapp.* **1** 153
[6] Wang H Y, Hu J, Xie Y Q, Chen J, Yu A, Wei X H, Dai Y M, Li M, Bao S L and Haacke E M 2013 *Chin. Phys. B* **22** 038702
[7] Yu S D, Wu S B and Xie Y Q 2013 *Comput. Math. Method M.* **2013** 202309
[8] Thireou T, Kontaxakis G, Strauss L G, Dimitrakopoulou-Strauss A, Pavlopoulos S and Santos A 2005 *Med. Biol. Eng. Comput.* **43** 23
[9] Zhu F, Rodriguez G D, Carpenter T, Atkinson M and Wardlaw J 2013 *IEEE J. Biomed. Health Inform.* **17** 950
[10] Haacke E M, Li M and Juvvigunta F 2013 *Magn. Reson. Imaging* **31** 481
[11] Lo E, Rogowska J, Bogorodzki P, Trocha M, Matsumoto K, Saffran B and Wolf G 1996 *J. Cerebr. Blood. F. Met.* **16** 60
[12] Boudraa A O, Behloul F, Janier M, Canet E, Champier J, Roux J P and Revel D 2001 *Comput. Biol. Med.* **31** 133
[13] Bai M, Hu K and Tang Y 2011 *Chin. Phys. B* **20** 128902
[14] Yu S D, Zhang R, Wu S B, Hu J and Xie Y Q 2013 *Biomed. Eng. Online* **12** 102
[15] Chavhan G B, Babyn P S, Thomas B, Shroff M M and Haacke E M 2009 *Radiographics* **29** 1433
[16] Andersen A H, Gash D M and Avison M J 1999 *Magn. Reson. Imaging* **17** 795
[17] Baumgartner R, Ryner L, Richter W, Summers R, Jarmasz M and Somorjai R 2000 *Magn. Reson. Imaging* **18** 89
[18] Faes L, Nollo G, Kirchner M, Olivetti E, Gaita F, Riccardi R and Antolini R 2001 *Med. Biol. Eng. Comput.* **39** 656